



Semiquantitative Analysis of Physiological Biodistribution of ⁶⁸Ga-DOTATATE and ⁶⁸Ga-DOTANOC

⁶⁸Ga-DOTATATE ve ⁶⁸Ga-DOTANOC'un Fizyolojik Biyodağılımının Semikantitatif Analizi

© Evrim SÜRER BUDAK¹, © Ali Ozan ÖNER², © Serkan DEMİRELLİ³, © Metin ERKILIÇ¹, © Adil BOZ¹, © Binnur KARAYALÇIN¹

¹Akdeniz University Faculty of Medicine, Department of Nuclear Medicine, Antalya, Turkey

²Afyon Kocatepe University Faculty of Medicine, Department of Nuclear Medicine, Afyonkarahisar, Turkey

³Denizli State Hospital, Clinic of Nuclear Medicine, Denizli, Turkey

Cite as: Sürer Budak E, Öner AO, Demirelli S, Erkılıç M, Boz A, Karayalçın B. Semiquantitative Analysis of Physiological Biodistribution of ⁶⁸Ga-DOTATATE and ⁶⁸Ga-DOTANOC. Forbes J Med 2023;4(2):116-25

ABSTRACT

Objective: In this study, we aimed to investigate the physiological biodistribution pattern of ⁶⁸Ga-DOTATATE and DOTANOC using standardized uptake value (SUV) parameters (maximum and mean) in nontumorous tissues on positron emission tomography/computed tomography (PET/CT) images.

Methods: Images of 40 patients (female, n=23 and male, n=17; mean age, 52.50±15.82 years) who had undergone ⁶⁸Ga-DOTA labeled (TATE or NOC) PET/CT imaging with the diagnosis of GEP-neuroendocrine tumor (NET), non-GEP-NET and thyroid cancer were retrospectively evaluated. SUV_{max} and SUV_{mean} measurements were performed from areas of physiologic uptake including pituitary gland, parotid and submandibular gland, palatine tonsils, thyroid, lungs, blood pool, thymus, lymph nodes, liver, pancreas (from head, body and tail parts), spleen, stomach, both adrenal gland, kidney, small bowel and colon, bone marrow, prostate, glandular breast tissue and muscle tissue.

Results: The highest uptake for ⁶⁸Ga-DOTATATE and ⁶⁸Ga-DOTANOC was noted in the spleen, adrenal, kidney, liver, pituitary gland and head of the pancreas, respectively. Lung, muscle, blood pool, bone marrow, lymph node and breast showed low uptake (SUV_{max-mean} <2), while moderate uptake was observed in the remaining organs.

Conclusion: We think that determination of uptake patterns and range of SUV_{max-mean} values for both agents in many organs will aid in discriminating between physiologic and pathologic uptake during the interpretation of images.

Keywords: ⁶⁸Ga-DOTATATE, ⁶⁸Ga-DOTANOC, PET/CT, somatostatin receptor, physiological biodistribution

ÖZ

Amaç: Bu çalışmada, ⁶⁸Ga-DOTATATE ve DOTANOC'un nontümöral dokulardaki fizyolojik biyodağılımının, pozitron emisyon tomografisi/bilgisayarlı tomografi (PET/BT) görüntülerinde standartlaştırılmış tutulum değeri (SUV) parametreleri (maksimum ve ortalama) kullanılarak araştırılması amaçlanmıştır.

Yöntem: GEP-nöroendokrin tümör (NET), non-GEP-NET ve tiroid kanseri tanısı ile ⁶⁸Ga-DOTA işaretli (TATE veya NOC) PET/BT görüntüleme yapılmış 40 hastanın (kadın: 23, erkek: 17; ortalama yaş: 52,50±15,82 yaş) görüntüleri retrospektif olarak değerlendirilmiştir. Hipofiz bezi, parotis, submandibular bez, palatin tonsil, tiroid, akciğer, kan havuzu, timus, lenf nodu, karaciğer, pankreas (baş, gövde ve kuyruk kesiminden), dalak, mide, adrenal bez (sağ ve sol), böbrek, ince ve kalın barsak, kemik iliği, prostat, meme glandüler dokusu ve kas dokuyu içerecek şekilde fizyolojik tutulum alanlarından SUV_{maks} ve SUV_{ort} ölçümleri yapılmıştır.

Received/Geliş: 30.05.2022

Accepted/Kabul: 03.09.2022

Corresponding Author/
Sorumlu Yazar:

Evrin SÜRER BUDAK MD,

Akdeniz University Faculty of
Medicine, Department of Nuclear
Medicine, Antalya, Turkey

Phone: +90 530 513 40 75

✉ evrimsurer@hotmail.com

ORCID: 0000-0002-8318-0785



Bulgular: ⁶⁸Ga-DOTATATE ve ⁶⁸Ga-DOTANOC için en yüksek tutulumlar sırasıyla dalak, adrenal bez, böbrek, karaciğer, hipofiz bezi ve pankreas baş kesiminden elde edilmiştir. Akciğer, kas dokusu, kan havuzu, kemik iliği, lenf nodu ve meme glanduler dokusunda düşük düzeyli tutulum ($SUV_{maks-ort} < 2$) saptanırken geriye kalan organlarda orta dereceli tutulum izlenmiştir.

Sonuç: Her iki ajan için de, pek çok organdaki tutulum paternleri ve $SUV_{maks-ort}$ değerlerinin bilinmesinin, görüntü analizi sırasında fizyolojik ve patolojik tutulum ayırımında faydalı olacağını düşünmekteyiz.

Anahtar Kelimeler: ⁶⁸Ga-DOTATATE, ⁶⁸Ga-DOTANOC, PET/BT, somatostatin reseptör, fizyolojik biyodağılım

INTRODUCTION

Neuroendocrine tumor (NET) cells characteristically overexpress somatostatin (SST) receptors (SSTRs).¹ SST is a peptide hormone that controls neurotransmission, hormone secretion, and cell proliferation by binding to SSTRs.² SSTRs have 5 subtypes (SSTR1-5); SSTR2 is the dominant form in NETs and in most of the normal tissues. SSTR overexpression enables functional imaging of NETs by positron emission tomography/computed tomography (PET/CT) using radiolabeled SST analogues.³ Gallium 68 1,4,7,10-tetraazacyclododecane-1,4,7,10-tetraacetic acid (⁶⁸Ga-DOTA) labeled SST analogues are commonly used in NET imaging. [⁶⁸Ga-DOTA-D-Phe1-Tyr3-octreotide (DOTATOC), DOTA-D-Phe1-Tyr3-octreotate (DOTATATE), DOTA-1-Nal3-octreotide (DOTANOC)] are the main SSTR analogues used in PET imaging. ⁶⁸Ga-labeled DOTA peptides consist of an active part directly bounding to SSTR (TATE, NOC, TOC), a chelating agent (DOTA) and a β emitter isotope (⁶⁸Ga). ⁶⁸Ga-DOTATATE shows selectively high affinity to SSTR2 while ⁶⁸Ga-DOTANOC has a wide spectrum binding profile for SSTR 2, 3 and 5. The maximum standardized uptake value (SUV_{max}) is a PET parameter that reflects the SSTR distribution and density. SSTR expression is not only specific to NETs. Many normal organs demonstrate variable SSTR expression, especially the pituitary gland, adrenals, kidneys, spleen and liver. It may be difficult to detect lesions in physiological uptake areas. Therefore, it is crucial to know the physiological biodistribution pattern of ⁶⁸Ga-DOTA SSTR analogs to discriminate pathological or physiological uptake on the onset of malignancy when interpreting PET/CT imaging. In the literature, many studies have shown the superiority of ⁶⁸Ga-DOTATATE and ⁶⁸Ga-DOTANOC in the diagnosis and treatment of NETs. However, there are limited data about physiological biodistribution in non-tumorous organs.⁴

In this study, we aimed to investigate the physiological biodistribution pattern of ⁶⁸Ga-DOTATATE and ⁶⁸Ga-DOTANOC by using SUV parameters (maximum and mean) in nontumorous tissues on PET/CT images of patients with the diagnosis of gastroenteropancreatic (GEP)-NET, non-GEP-NET, and thyroid cancer.

METHODS

Patient population: ⁶⁸Ga-DOTATATE (n=25) and ⁶⁸Ga-DOTANOC (n=15) PET/CT images of 40 patients with the

diagnosis of GEP-NET (n=11, 27.5%), non-GEP-NET (n=14, 35%) and thyroid cancer (n=15, 37.5%) were evaluated retrospectively. The medical records of each patient were examined. Patients with documented or suspicious additional malignancies were excluded. The study was approved by the Akdeniz University Faculty of Medicine of Local Ethics Committee (decision number: 85, date: 09.04.2013).

⁶⁸Ga-DOTA Imaging: ⁶⁸Ga-DOTATATE and ⁶⁸Ga-DOTANOC (Advanced Biochemical Compound (ABX), Germany) were labeled using a tin-oxide-based fully automated system (GallElute, Scintomics, Fürstfeldbruck, Germany) using a standardized labeling sequence. Radiochemical purity was over 97% in all cases based on high-performance liquid chromatography. The average doses of intravenously (IV) administered ⁶⁸Ga-DOTATATE and ⁶⁸Ga-DOTANOC were 132.05 MBq and 116.77 MBq, respectively. Whole-body images from the skull base to mid-thigh were acquired 60±10 minutes after the injection using a hybrid PET/CT scanner (Biograph True Point, Siemens Medical Solutions, Germany). A low-dose 16-slice multidetector CT scan (parameters: 26 mA, 120 kV, table speed 0.5sec/rotation 80 mA, 140 kV, 27 mm/rotation, and slice width of 5.0 mm) was used for screening. A standard whole-body PET scan was conducted in a 3D mode with an acquisition time of 3 min per bed position scanning the exact area with the CT scan. PET images were reconstructed with and without correction for attenuation using an "attenuation-weighted ordered subset expectation maximization" (AWOSEM) algorithm. Then, the data were transferred into a Syngo TrueD workstation (Siemens Medical Solutions) for further processing.

Image analysis: PET, CT, and fused/CT images in the axial, sagittal, and coronal planes and maximum intensity projection (MIP) images were reviewed and analyzed by a single nuclear medicine specialist. Measurements were performed from areas of physiologic uptake including pituitary gland, parotid gland, submandibular gland, palatine tonsil, thyroid, lung, blood pool (left ventricular cavity), thymus (if visualized), lymph nodes (axillary region with benign morphological characteristics), liver, pancreas (head, body and tail), spleen, stomach (fundus and other parts), adrenal gland (left-right), kidney (renal cortex), small bowel and colon (areas where lumen and wall can be separately discerned), bone marrow (iliac crest), prostate,

glandular breast tissue and muscle tissue (gluteal muscle). If the primary diagnosis was related to one of these physiologic organs, this organ was excluded. A volume of interest (ROI) was drawn in the transaxial attenuation-corrected PET slice with correlation with CT images in order to fit the organ and avoid any scatter from adjacent tissues. ROIs are drawn including whole organ in small structures such as pituitary gland and adrenals, while approximately 2 cm circular for larger organs. The homogeneous/less heterogeneous uptake pattern without any intense focus was especially preferred while fitting ROIs. SUV_{max} and mean standardized uptake (SUV_{mean}) values were calculated from ROIs. SUV_{mean} was taken as the average SUV concentration in ROI. SUV_{max} and SUV_{mean} values were automatically provided by a computer - assisted software on the basis of a standardized formula.

Statistical Analysis

For statistical analysis Statistical Package for Social Sciences 19.0 was used. The fitness of variables to normal distribution was analyzed using the Shapiro-Wilk test. For the analysis of correlations between nominal variables, chi-square test, for the comparison of two independent groups, according to characteristics of the data, t-test or Mann-Whitney U test was used. For the comparison of two and three dependent groups, Wilcoxon signed-ranks test and Freidman test were used, respectively. As post-hoc analysis, Wilcoxon signed rank test and Bonferroni correction were employed. P values less than level 0.05 were considered significant.

RESULTS

Patient characteristics: Patient characteristics are summarized in Table 1. No statistically significant difference was detected between ^{68}Ga -DOTATATE and ^{68}Ga -DOTANOC groups characteristics for gender, age, activity injected, and time of examination.

Physiologic uptake patterns: Number of evaluated organs were as follows: pituitary gland (n=40), palatine tonsil (n=40), submandibular gland (n=40), parotid gland (n=40), lungs (n=40), kidney (n=40), small bowel (n=40), colon (n=40), lymph node (n=40), breast (n=40), muscle (n=40), bone marrow (n=40), blood pool (n=40), spleen (n=39), right adrenal (n=39), left adrenal (n=38), pancreas (head, body and tail, n=36), liver (n=35), stomach (fundus and other, n=32), thyroid (n=25), prostate (n=17) and thymus (n=16). One patient was splenectomized (n=39) and thymic uptake was observed only in 16 patients, who are relatively at younger ages (16-23 years old). The highest uptake for ^{68}Ga -DOTATATE and ^{68}Ga -DOTANOC was noted in spleen, adrenal, kidney, liver, pituitary gland and head of the pancreas, respectively. Lung, muscle, blood pool, bone marrow, lymph node and breast showed low uptake ($SUV_{max-mean} < 2$) while moderate uptake was observed in the remaining organs (palatine tonsil, submandibular gland, parotid gland, thyroid, thymus, body and tail of the pancreas, stomach, small bowel, colon and prostate). Whole body MIP images demonstrating the physiological biodistribution of ^{68}Ga -DOTATATE and ^{68}Ga -DOTANOC are shown in Figure 1. The SUV_{max} and SUV_{mean} values (mean and standard deviation) of reference organs

Table 1. Patient characteristics in ^{68}Ga -DOTATATE and ^{68}Ga -DOTANOC groups

	^{68}Ga -DOTATATE	^{68}Ga -DOTANOC
Gender	F: 15 M: 10	F: 8 M: 7
Age	Mean: 51.44±11.17 Median: 53.00 Min-max: 16-76	Mean: 54.27±17.25 Median: 56.00 Min-max: 19-84
Diagnosis	Gastric NET: 6 (4 F, 2 M) Appendix NET: 1 (M) Carcinoma of unknown primary origin: 4 (4 M) Carcinoid syndrom: 1 (M) Paraganglioma: 2 (2 F) Pheochromocytoma : 1 (M) Medullary thyroid carcinoma: 4 (4 F) Follicular thyroid carcinoma: 3 (3 F) Hurthle cell+papillary thyroid carcinoma: 1 F Papillary thyroid carcinoma: 2 (1 F, 1 M)	Gastric NET: 2 (1 F, 1 M) Pancreatic NET: 2 (1 F, 1 M) Carcinoma of unknown primary origin: 4 (1 F, 3 M) Ectopic cushing syndrome: 1 (F) Cerviks NET: 1 (F) Medullary thyroid carcinoma: 1 (M) Hurthle cell thyroid carcinoma: 1 (M) Papillary thyroid carcinoma: 3 (3 F)
Injected dose (MBq)	Mean: 132.05±28.64 Median: 142.45 Min-max: 62.16-198.32	Mean: 116.77±28.30 Median: 111.00 Min-max: 85.10-186.11
Imaging interval (minute)	Mean: 63.64±19.70 Median: 57.00 Min-max: 37-125	Mean: 60.87±16.12 Median: 56.00 Min-max: 39-85

F: Female, M: Male, Min-max: Minimum-maximum, NET: Neuroendocrine tumor

and p values of organs showing statistically significant uptake in the ^{68}Ga -DOTATATE and ^{68}Ga -DOTANOC groups are shown in Tables 2 and 3.

Focal, diffuse, and homogenous uptake was observed in the pituitary gland. In the ^{68}Ga -DOTATATE group, statistically significantly higher SUV_{max} and SUV_{mean} values were detected ($p=0.007$ and $p=0.003$, respectively).

Spleen showed homogeneous and highest uptake without a statistically significant difference between ^{68}Ga -DOTATATE and ^{68}Ga -DOTANOC for SUV_{max} and SUV_{mean} values ($p=0.989$ and $p=0.945$, respectively).

Uptake in the liver was heterogeneous and significantly higher in the ^{68}Ga -DOTATATE group for both SUV_{max} and SUV_{mean} values ($p=0.001$ and $p<0.001$, respectively).

Heterogeneous uptake was observed in the pancreas; moderate for body and tail, while high for head. The pancreatic head showed significantly higher uptake than the body and tail for both ^{68}Ga -DOTATATE ($p<0.001$) and ^{68}Ga -DOTANOC ($p=0.002$). However, in the head of pancreas and between the body and tail of the pancreas, no significant difference was observed.

Diffuse and intense cortical uptake was observed in kidneys, which was significantly higher for ^{68}Ga -DOTATATE SUV_{max} and SUV_{mean} values ($p=0.008$ and $p<0.001$, respectively).

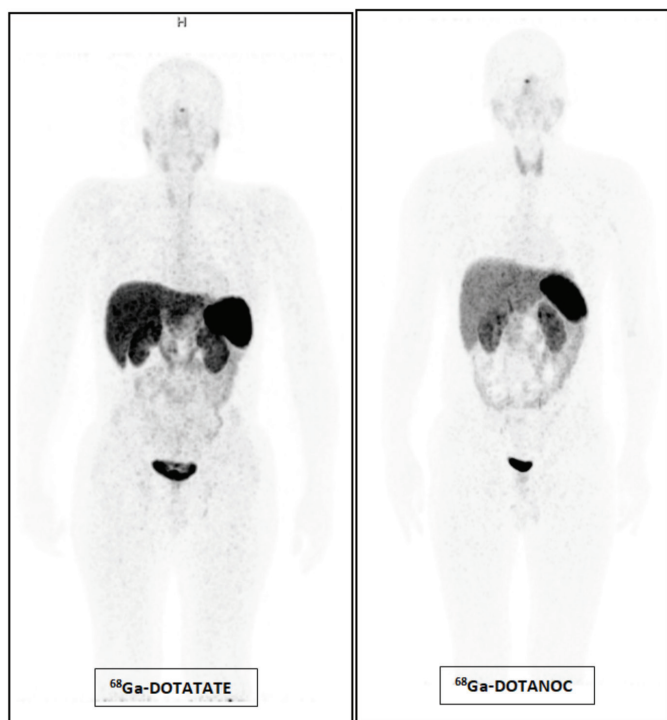


Figure 1. Whole body MIP images demonstrating physiologic biodistribution of ^{68}Ga -DOTATATE and ^{68}Ga -DOTANOC

MIP: Maximum intensity projection

Adrenal glands showed symmetrical, mostly triangular diffuse uptake with no significant difference between two sides (right-left) and two agents (^{68}Ga -DOTATATE and ^{68}Ga -DOTANOC).

Moderate uptake was observed in the stomach. Significantly higher SUV_{max} and SUV_{mean} values were observed in the gastric fundus in ^{68}Ga -DOTATATE ($p=0.001$ and $p<0.001$, respectively) and ^{68}Ga -DOTANOC groups ($p=0.002$ and $p=0.007$, respectively).

The intestinal and colonic uptake was patchy. Significantly higher SUV_{max} and SUV_{mean} values were obtained in the ^{68}Ga -DOTATATE group (for intestine $p<0.001$; for colon $p=0.035$ and $p=0.026$, respectively).

Palatine tonsils ($p=0.41$ and $p=0.074$, respectively), submandibular gland ($p<0.001$), and parotid gland ($p<0.001$) showed symmetric and moderate uptake, which was significantly higher in ^{68}Ga -DOTATATE than in palatine tonsils.

A predominantly diffuse uptake was observed in the thyroid gland (Figure 2). These cases were correlated with CT images, which did not show any abnormality such as nodules or heterogeneity. Thyroid function tests were also within normal limits. In the ^{68}Ga -DOTATATE group, SUV_{max} and SUV_{mean} values were significantly higher than ^{68}Ga -DOTANOC group ($p=0.01$, and $p=0.007$, respectively).

In cases where the thymus can be visualized, generally homogenous and low-moderate uptake was observed, as in prostate (heterogenous). Because of the scarce number of cases, statistical analysis could not be performed.

Lower levels of uptake were observed in the lung, lymph node, muscle, bone marrow, blood pool, and breast tissue. Muscle ($p=0.012$ and $p=0.020$, respectively) and bone marrow ($p<0.001$) showed significantly higher SUV_{max} and SUV_{mean} values in ^{68}Ga -DOTATATE group, while no significant

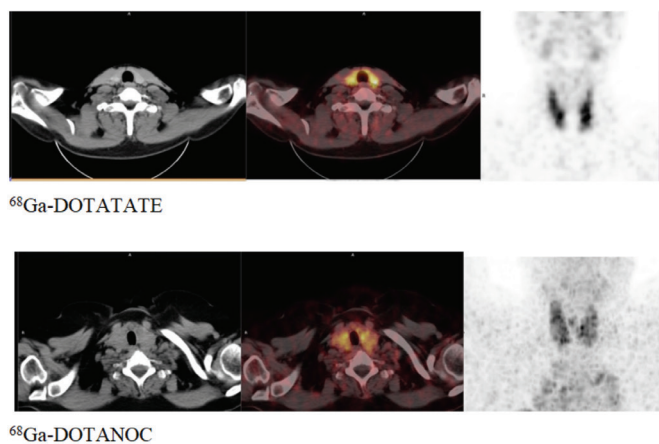


Figure 2. Thyroid uptake in ^{68}Ga -DOTATATE and ^{68}Ga -DOTANOC images

difference was observed in breast tissue (p=0.376). Lymph node SUV_{max} values were also higher in ⁶⁸Ga-DOTATATE group (p=0.018).

Only blood pool (p=0.024 and p=0.009, respectively) and lung (p=0.018 ve p=0.043, respectively) SUV_{max} and SUV_{mean} showed significantly higher uptake in ⁶⁸Ga-DOTANOC group.

DISCUSSION

As ⁶⁸Ga-DOTATATE and ⁶⁸Ga-DOTANOC PET/CT are increasingly used in NET imaging, knowing the physiological distribution pattern is becoming more important to prevent misdiagnosis. In this study, the biodistribution of ⁶⁸Ga-DOTATATE and ⁶⁸Ga-DOTANOC in normal healthy organs

was semiquantitatively evaluated using SUV_{max} and SUV_{mean} parameters. Our goal is to determine a reference value that will aid in the discrimination between physiologic and pathologic uptakes, especially in the gray zone.

In our study, the highest uptake values for ⁶⁸Ga-DOTATATE and ⁶⁸Ga-DOTANOC were detected in the spleen, adrenal glands, kidney, liver, pituitary gland, and head of the pancreas, respectively.

The pituitary gland showed significantly higher SUV_{max} and SUV_{mean} values for ⁶⁸Ga-DOTATATE than ⁶⁸Ga-DOTANOC (p=0.007 and p=0.003 respectively) compatible with the recent literature.⁵⁻⁷ But in our study, obtained median SUV_{max} and SUV_{mean} values for ⁶⁸Ga-DOTATATE were significantly higher as compared with the results of Kunikowska et al.⁵

Table 2. SUV_{max} values of reference organs and p values of organs showing statistically significant uptake in the ⁶⁸Ga-DOTATATE and ⁶⁸Ga-DOTANOC groups

Organ	SUV _{max}										Statistically significant p values
	⁶⁸ Ga-DOTATATE					⁶⁸ Ga-DOTANOC					
	(n)	Mean	SD	Median	Min-max	(n)	Mean	SD	Median	Min-max	
Pituitary gland	25	13.73	4.66	13.96	3.55-22.33	15	9.68	5.29	7.96	3.21-22.75	p=0.007
Palatine tonsils	25	3.35	1.54	3.01	1.43-7.13	15	2.52	0.95	2.28	1.11-4.47	
Submandibular gland	25	3.75	1.34	3.66	1.7-6.60	15	2.13	0.53	2.08	1.21-3.30	p<0.001
Parotid gland	25	3.50	1.72	3.61	0.76-7.36	15	1.90	0.65	1.87	0.88-3.01	p<0.001
Thyroid	15	7.54	3.15	7.60	2.03-11.84	10	3.96	1.75	4.03	1.90-7.61	p=0.01
Thymus	12	2.40	1.01	2.04	1.18-4.19	4	2.37	1.04	2.09	1.47-3.82	
Lung	25	0.53	0.23	0.47	0.17-1.25	15	0.73	0.31	0.73	0.23-1.40	p=0.018
Liver	22	14.20	3.69	13.97	6.81-23.18	13	10.17	2.44	10.60	6.25-14.12	p=0.001
Spleen	24	32.77	9.20	33.94	12.07-47.65	15	32.73	11.18	31.65	8.76-55.24	
Pancreas-head	24	9.62	4.11	8.11	5.82-24.68	12	9.07	3.49	8.40	4.88-16.79	
Pancreas-body	24	4.89	1.68	4.99	2.52-9.04	12	3.38	1.10	3.17	1.89-5.96	p=0.004
Pancreas-tail	24	5.33	1.60	5.05	2.3-8.47	12	3.65	1.31	3.53	1.89-6.73	p=0.001
Stomach-fundus	19	8.15	3.53	8.29	1.56-14.74	13	4.47	1.83	4.16	2.56-9.08	p=0.001
Stomach-other	19	6.35	3.07	5.80	0.90-12.14	13	3.23	1.07	2.95	2.09-5.38	p=0.001
Kidney	25	15.26	4.20	15.07	6.47-24.02	15	11.76	3.12	11.94	4.89-16.56	p=0.008
Adrenal gland-right	24	14.62	4.61	14.98	8.19-27.41	15	15.33	6.41	13.84	5.78-31.96	
Adrenal gland-left	23	16.57	5.58	15.21	7.17-27.85	15	16.60	5.17	15.76	6.16-25.91	
Small bowel	25	3.83	1.07	3.44	2.60-6.74	15	2.58	0.88	2.47	1.18-4.81	p<0.001
Colon	25	4.44	3.30	2.75	1.62-11.06	15	2.60	1.51	2.39	1.15-6.99	p=0.035
Prostate	10	7.28	2.99	7.01	3.24-11.98	7	5.80	2.65	4.77	2.95-9.20	
Lymph node	25	1.77	0.75	1.56	0.55-4.06	15	1.28	0.36	1.25	0.74-1.98	p=0.018
Glandular breast tissue	25	1.01	0.52	0.99	0.27-2.28	15	0.86	0.43	0.71	0.31-1.79	
Muscle tissue	25	1.19	0.46	1.05	0.53-2.10	15	0.87	0.30	0.83	0.35-1.37	p=0.012
Bone marrow	25	1.97	0.72	2.16	0.74-3.13	15	1.08	0.29	1.10	0.70-1.80	p<0.001
Blood pool	25	0.99	0.40	0.90	0.41-1.95	15	1.27	0.28	1.25	0.77-1.77	p=0.024

SD: Standard deviation, Min-max: Minimum-maximum

and Kabasakal et. al.⁷ In the pituitary gland, SSTR2 and SSTR5 are predominantly expressed subtypes especially in the anterior lobe.⁸ Selectively higher affinity of ⁶⁸Ga-DOTATATE to SSTR2 can explain significantly higher levels in pituitary gland. Our SUV_{max} values for ⁶⁸Ga-DOTANOC were also significantly higher than those of Prasad and Baum.⁹

In vitro studies have demonstrated that hepatocytes and hepatic stellate cells do not express any SSTR subtypes.¹⁰ Boy et al.¹¹ reported that the main SSTR subtype in liver is SSTR1 (94.2%), followed by SSTR2 (5.7%) and SSTR5 (0.1%), while negative for SSTR3 and SSTR4. To an accepted consensus, the uptake of ⁶⁸Ga-DOTATATE and ⁶⁸Ga-DOTANOC in the liver is related to the metabolism and

elimination of peptides. In our study, liver SUV_{max} and SUV_{mean} values for ⁶⁸Ga-DOTATATE were significantly higher than ⁶⁸Ga-DOTANOC (p=0.001 and p<0.001 respectively), which is in accordance with the literature data.⁵⁻⁷

In our study the highest uptake levels for ⁶⁸Ga-DOTATATE and ⁶⁸Ga-DOTANOC were observed in spleen, which shows no significant intergroup difference. Kabasakal et al.⁷ reported comparable results with our study. In the spleen, predominantly receptor subtype is SSTR2.¹¹ Our SUV_{max} and SUV_{mean} values for ⁶⁸Ga-DOTATATE were significantly higher than the literature.^{5,7} Our SUV_{max} values for ⁶⁸Ga-DOTANOC were also significantly higher than those indicated by Prasad and Baum.⁹

Table 3. SUV_{mean} values of reference organs and p values of organs showing statistically significant uptake in the ⁶⁸Ga-DOTATATE and ⁶⁸Ga-DOTANOC groups

Organ	SUV _{mean}										Statistically significant p values
	⁶⁸ Ga-DOTATATE					⁶⁸ Ga-DOTANOC					
	(n)	Mean	SD	Median	Min-max	(n)	Mean	SD	Median	Min-max	
Pituitary gland	25	10.07	3.62	9.24	2.68-16.67	15	6.77	3.43	5.88	2.50-14.02	p=0.003
Palatine tonsils	25	2.77	1.26	2.65	1.27-5.47	15	1.96	0.67	1.72	1.08-3.32	
Submandibular gland	25	2.95	1.05	3.08	1.49-5.41	15	1.58	0.34	1.53	1.06-2.41	p<0.001
Parotid gland	25	2.79	1.48	2.79	0.67-6.27	15	1.41	0.43	1.41	0.77-2.07	p<0.001
Thyroid	15	6.27	2.69	6.16	1.42-9.56	10	3.14	1.39	3.19	1.46-5.66	p=0.007
Thymus	12	1.68	0.54	1.61	0.96-2.88	4	1.63	0.62	1.55	1.01-2.42	
Lung	25	0.35	0.15	0.32	0.14-0.79	15	0.48	0.20	0.52	0.16-0.86	p=0.043
Liver	22	10.62	2.67	10.19	5.34-18.16	13	7.45	1.59	7.20	4.94-10.38	p<0.001
Spleen	24	27.98	8.31	28.29	8.09-44.83	15	27.77	10.61	25.97	7.34-51.64	
Pancreas-head	24	7.34	2.78	6.28	4.38-17.03	12	6.70	2.26	6.25	4.22-11.92	
Pancreas-body	24	3.78	1.23	3.69	1.57-6.73	12	2.54	0.90	2.45	1.29-4.22	p=0.002
Pancreas-tail	24	4.39	1.37	4.07	1.74-7.08	12	3.03	1.19	2.83	1.47-6.10	p=0.001
Stomach-fundus	19	6.88	3.06	6.80	1.08-12.51	13	3.36	1.00	3.52	2.01-5.39	p<0.001
Stomach-other	19	4.86	2.43	4.40	0.77-9.60	13	2.53	0.67	2.44	1.57-3.78	p<0.001
Kidney	25	13.05	3.54	12.68	6.07-19.94	15	8.77	2.85	9.00	3.64-13.23	p<0.001
Adrenal gland-right	24	12.07	3.81	12.27	7.24-23.25	15	11.93	4.40	12.10	4.08-22.34	
Adrenal gland-left	23	14.11	4.91	13.98	6.47-25.90	15	12.66	4.11	11.91	4.57-21.05	
Small bowel	25	3.15	0.82	3.09	2.17-5.25	15	2.17	0.70	2.56	1.10-4.04	p<0.001
Colon	25	3.58	2.55	2.23	1.37-8.52	15	1.97	0.80	1.69	1.02-4.11	p=0.026
Prostate	10	5.31	2.42	4.63	1.97-8.78	7	3.78	1.65	3.19	2.19-6.33	
Lymph node	25	1.19	0.50	1.05	0.40-2.60	15	0.88	0.23	0.92	0.52-1.28	
Glandular breast tissue	25	0.70	0.38	0.63	0.20-1.69	15	0.61	0.35	0.54	0.21-1.40	
Muscle tissue	25	0.87	0.32	0.80	0.49-1.60	15	0.64	0.23	0.57	0.26-1.15	p=0.020
Bone marrow	25	1.61	0.58	1.75	0.62-2.52	15	0.86	0.24	0.84	0.57-1.53	p<0.001
Blood pool	25	0.70	0.29	0.63	0.29-1.41	15	0.94	0.23	0.93	0.60-1.42	p=0.009

SD: Standard deviation, Min-max: Minimum-maximum

In the head of the pancreas, SUV_{max} and SUV_{mean} values for both ^{68}Ga -DOTATATE and ^{68}Ga -DOTANOC did not show any significant intergroup difference. Conversely, in the body and tail of the pancreas, SUV_{max} and SUV_{mean} values for ^{68}Ga -DOTATATE were significantly higher than ^{68}Ga -DOTANOC group. When the regional distribution pattern (head, body and tail) was considered, SUV_{max} and SUV_{mean} values of both ^{68}Ga -DOTATATE and ^{68}Ga -DOTANOC groups were significantly higher in the head than in the body and tail. However, SUV_{max} and SUV_{mean} values of body and tail did not show any significant intergroup difference for both agents. Although the pancreas contains all 5 SSTR subtypes, especially in α and β cells, predominantly expression of SSTR2 has been demonstrated. Less frequently SSTR1 and SSTR5 are also expressed.^{12,13} Boy et al.¹¹ reported the pancreatic expression rates of SSTR1 (47.9%), SSTR5 (46.8%), SSTR2 (5%), and SSTR3 (9.3%) while negative for SSTR4 (0.0%). However, regional distribution patterns of SSTRs were not indicated. We think that although SSTR2 expression is lower than SSTR5 in the pancreatic head, selective and higher affinity of ^{68}Ga -DOTATATE to SSTR2 compensates for this discrepancy, which might be an explanation for similar uptake levels of these two agents in the pancreatic head. Since islet cells can be seen in any region in clusters, focal areas of increased uptake can be considered as a variant of physiologic distribution, but precaution should still be exercised. Currently another subject of debate in the literature is pancreatic polypeptide (PP) cells of the pancreas. PP cells are pancreatic islet cells as alpha, beta, and delta cells. Immunohistochemical studies have demonstrated that these cells are localized in the head of the pancreas and especially around the uncinate process.¹⁴ It has also been demonstrated that areas rich in PP cells contain a lesser number of alpha and beta cells compared with the body and tail of the pancreas. This issue is being debated in literature studies, up to now, any study that has demonstrated whether PP cells express SSTR has not been performed. However, studies that demonstrate the correlation between PP cells and SSTR expression can clarify diffuse uptake observed in the head of the pancreas. In our study, higher ^{68}Ga -DOTATATE SUV_{max} and SUV_{mean} values for the head of the pancreas were correlating with the data of Kunikowska et al.⁵ and Kuyumcu et al.⁶ In our study, significantly higher SUV_{max} values for ^{68}Ga -DOTANOC were detected in the head of the pancreas when compared with the study of Prasad and Baum.⁹

SUV_{max} and SUV_{mean} values for ^{68}Ga -DOTATATE and ^{68}Ga -DOTANOC did not show a significant differences for the right and left adrenal glands separately. However, the ^{68}Ga -DOTATATE SUV_{mean} value for the left adrenal gland was found to be significantly higher relative to the right adrenal

gland ($p=0.039$). Boy et al.¹¹ demonstrated the adrenal SSTR expression rates as follows: SSTR5 (54.3%), SSTR2 (33.0%), SSTR1 (10.5%), SSTR3 (2.2%), and SSTR4 (0.0%). Despite the intense expression of SSTR5 in adrenal gland, it was thought that the higher and more selective affinity of ^{68}Ga -DOTATATE to SSTR2 versus ^{68}Ga -DOTANOC will compensate this difference and possibly explain the similar uptake rates of both groups. SSTR2 and SSTR5 are the most common receptor types in adrenal glands, which explain the second highest uptake for both agents. Kabasakal et al.⁷ reported no statistically significant difference for SUV_{max} values of ^{68}Ga -DOTATATE and ^{68}Ga -DOTANOC compatible with our study. Kunikowska et al.⁵ reported similar results for ^{68}Ga -DOTATATE SUV_{max} and SUV_{mean} values for the right adrenal and SUV_{max} values for the left adrenal. However, SUV_{mean} values of the left adrenal gland were significantly higher in our study (SUV_{mean} : 14.11 ± 4.91 vs 10.10 ± 3.80 , $p=0.002$). They also reported higher adrenal SUV_{max} values for ^{68}Ga -DOTATATE than ^{68}Ga -DOTANOC (14.6 vs 6).

SUV_{max} and SUV_{mean} values for renal uptake of ^{68}Ga -DOTATATE were significantly higher than ^{68}Ga -DOTANOC group. Kidneys express all 5 subtypes of SSTR, mostly in distal nephrons and collecting tubuli. Vasa recta diffusely expresses SSTR2, while expressions of SSTR1 and SSTR2 were seen in glomeruli and collecting tubuli; proximal tubuli mostly express SSTR3, SSTR4 and SSTR5.¹⁵ Because of its hydrophilic structure, ^{68}Ga -DOTATATE is excreted from kidneys. The highest third uptake and higher uptake of ^{68}Ga -DOTATATE in kidneys have been thought to be related to the metabolism of these agents and diffuse SSTR2 expression. Our SUV_{max} and SUV_{mean} values for renal ^{68}Ga -DOTATATE uptake were comparable with the literature data.^{5,6} However, SUV_{max} values for ^{68}Ga -DOTANOC were significantly lower than the values of Prasad and Baum⁹ (11.76 ± 3.12 vs 12.90 ± 3.80 , $p=0.032$).

In the stomach, uptake was investigated in two parts; fundus, and other. Both in the fundus and other parts; SUV_{max} and SUV_{mean} values for ^{68}Ga -DOTATATE were significantly higher than ^{68}Ga -DOTANOC. Also, SUV_{max} and SUV_{mean} values for ^{68}Ga -DOTATATE group were significantly higher for the fundus than for other parts. SSTR1 is the dominant subtype in gastric mucosa; immunohistochemical studies have demonstrated diffuse SSTR2 expression in gastric cells, especially in the fundus.¹⁶ This finding supports the significantly higher ^{68}Ga -DOTATATE uptake rates in the stomach. Physiological stomach uptake has rarely been investigated. Shastry et al.⁴ and Özgüven et al.² reported similar SUV_{max} values for ^{68}Ga -DOTATATE in accordance with our study.

SUV_{max} and SUV_{mean} values of both small and large intestine for ^{68}Ga -DOTATATE were significantly higher than ^{68}Ga -

DOTANOC. SSTR2 overexpression has been demonstrated in mucosal neuroendocrine cells, submucosa, myenteric plexus and solitary lymphoid follicles along the gastrointestinal (GI) tract in *in vivo* studies.^{16,17} The presence of diffuse SSTR2 and lower levels of SSTR3 and SSTR5 expression have also been reported in the vessels of inflammatory areas of the GI tract.¹⁸ All of these can explain the patchy, variable ^{68}Ga -DOTATATE uptake observed in the intestine. Variable uptake may also be related to intestinal motility and movement artifacts on PET/CT fusion images.

Pulmonary uptake was minimal for both agents. Significantly higher SUV_{max} and SUV_{mean} values were observed in ^{68}Ga -DOTATATE group. Normal lung tissue mainly expresses SSTR4.¹⁹ However, SSTR4 does not have affinity for ^{68}Ga -DOTATATE and ^{68}Ga -DOTANOC. SSTR2 is expressed in various components of lung inflammation, such as epithelial cells, inflammatory cells, and fibroblasts, which may explain the more intensive uptake of ^{68}Ga -DOTATATE.¹⁹ In our study, pulmonary ^{68}Ga -DOTATATE and ^{68}Ga -DOTANOC SUV_{max} values were similar to the data of Kuyumcu et al.⁶ and Prasad and Baum.⁹

In palatine tonsils, SUV_{max} and SUV_{mean} values for ^{68}Ga -DOTATATE and ^{68}Ga -DOTANOC did not show any significant difference. In *in vitro* studies, SSTR2 expression was demonstrated in palatine tonsils.²⁰ In the literature, Shastry et al.⁴ reported ranges of SUV_{max} values for palatine tonsils between 0.8 and 3.8 (mean: 2.3).

In salivary glands such as the submandibular and parotid glands, SUV_{max} and SUV_{mean} values were significantly higher for ^{68}Ga -DOTATATE group. Salivary glands mainly express SSTR2 (60%).¹¹ Our data are compatible with the literature.^{5,6}

The thyroid gland showed significantly higher SUV_{max} and SUV_{mean} values in ^{68}Ga -DOTATATE group. All patients were euthyroid, and no thyroid nodules were detected in correlating CT images. Uptake was diffuse, homogenous, and varied on a wide scale, which complies with variable SSTR2 expression demonstrated in *in vitro* studies. Boy et al.¹¹ reported thyroidal expressions of SSTR1, SSTR2, and SSTR5 as 54%, 44.2% and 0.7%, respectively. The dominance of SSTR2 in the thyroid gland accounts for significantly higher ^{68}Ga -DOTATATE uptake rates. SSTR2 overexpression in thyroid tumors is also documented.²¹ Therefore, focal ^{68}Ga -DOTATATE uptake in the thyroid gland should be further examined for the presence of a potential malignancy. In our study, ^{68}Ga -DOTATATE SUV_{max} values are much higher than literature data while similar for ^{68}Ga -DOTANOC.^{2,4,5,9}

Lymph nodes revealed significantly higher SUV_{max} values in ^{68}Ga -DOTATATE group but SUV_{mean} values did not differ between two groups. Studies demonstrated marked SSTR2 mRNA expression in the germinal centers of activated

lymphocytes.¹⁸ Shastry et al.⁴ reported much lower nodal ^{68}Ga -DOTATATE SUV_{max} values than us.

In our study, measurements were performed from gluteal muscle similar to Prasad and Baum⁹ and similarly found significantly higher SUV_{max} (and additional SUV_{mean}) values in ^{68}Ga -DOTATATE group. Muscle tissue is known to express SSTR1, SSTR2 and SSTR5 as 88.9%, 10.1% and 0.3%, respectively, which may be an explanation for increased ^{68}Ga -DOTATATE uptake.¹¹

Blood pool measurements were performed from the left ventricular cavity. SUV_{max} and SUV_{mean} values were significantly higher in the ^{68}Ga -DOTANOC group. Granulocytes and erythrocytes do not express SSTRs. In peripheral blood, B and T lymphocytes express only SSTR3, and monocytes can express SSTR2 when activated.²² We had similar ^{68}Ga -DOTATATE and ^{68}Ga -DOTANOC SUV_{max} values with the literature.^{4,9}

Bone marrow measurements were obtained from the iliac crest. SUV_{max} and SUV_{mean} values for ^{68}Ga -DOTATATE were significantly higher than ^{68}Ga -DOTANOC. Precursor cells in bone marrow express SSTR2.²² Compatible with our results, Boy et al.¹¹ reported 70.1% SSTR2 and 0.5% SSTR5 expression in bone marrow specimens.

In breast tissue, SUV_{max} and SUV_{mean} values did not reveal significant differences between the two groups.

The measurements from the prostate and thymus were also obtained; however, statistical evaluation could not be performed due to the scarce number of cases.

Generally, dominance of ^{68}Ga -DOTATATE detected in our study can be associated with dominant SSTR2 overexpression of most tissues and markedly higher binding affinity of ^{68}Ga -DOTATATE over ^{68}Ga -DOTANOC.²³⁻²⁵ When compared with the literature, in our study pituitary gland, liver and spleen revealed significantly higher SUV_{max} and SUV_{mean} values for both agents. Although the similar injected doses, examination timing and amounts of labeled peptide molecules; higher uptake rates are thought to be related to the differences in labeling systems (manual/semi-automatic/fully automatic) and specific activities (not assessed in our study). In our study, the distribution of ^{68}Ga -DOTATATE and ^{68}Ga -DOTANOC uptake rates between genders could not be evaluated due to the inadequate number of patients.

Study Limitations

This study has limitations such as the scarce number of patients involved in the study. The the number of patients in the two groups was not similar (25 patients in ^{68}Ga -DOTATATE group vs 15 patients in ^{68}Ga -DOTANOC group). Although the results are mostly compatible with

the literature, studies with a larger number of patients are needed to generalize the results.

CONCLUSION

Despite the large number of studies that show the superiority of ⁶⁸Ga-DOTATATE and ⁶⁸Ga-DOTANOC in the diagnosis and management of NET, very scarce data are available on biodistribution of physiological uptake in non-tumoral organs. This study used SUV_{max} and SUV_{mean} values to semiquantitatively demonstrate the distribution pattern of ⁶⁸Ga-DOTATATE and ⁶⁸Ga-DOTANOC in normal organs. We think that determination of uptake patterns and range of SUV values we defined for both agents in many organs will aid in discrimination between physiologic and pathologic uptake during interpretation of images.

Ethics

Ethics Committee Approval: The study was approved by the Akdeniz University Faculty of Medicine of Local Ethics Committee (decision number: 85, date: 09.04.2013).

Informed Consent: Retrospective study.

Peer-review: Externally peer-reviewed.

Authorship Contributions

Concept: E.S.B., M.E., A.B., B.K., Design: E.S.B., M.E., A.B., B.K., Data Collection or Processing: E.S.B., A.O.Ö., S.D., Analysis or Interpretation: E.S.B., M.E., A.B., B.K., Literature Search: E.S.B., Writing: E.S.B.

Conflict of Interest: No conflict of interest was declared by the authors.

Financial Disclosure: The authors declared that this study received no financial support.

REFERENCES

- Schaer JC, Waser B, Mengod G, Reubi JC. Somatostatin receptor subtypes sst1, sst2, sst3 and sst5 expression in human pituitary, gastroentero-pancreatic and mammary tumors: comparison of mRNA analysis with receptor autoradiography. *Int J Cancer*. 1997;70:530-7.
- Özgülven S, Filizoğlu N, Kesim S, et al. Physiological Biodistribution of ⁶⁸Ga-DOTA-TATE in Normal Subjects. *Mol Imaging Radionucl Ther*. 2021;30:39-46.
- Zamora V, Cabanne A, Salanova R, et al. Immunohistochemical expression of somatostatin receptors in digestive endocrine tumours. *Dig Liver Dis*. 2010;42:220-5.
- Shastri M, Kayani I, Wild D, et al. Distribution pattern of ⁶⁸Ga-DOTATATE in disease-free patients. *Nucl Med Commun*. 2010;31:1025-32.
- Kunikowska J, Królicki L, Pawlak D, Zerizer I, Mikołajczak R. Semiquantitative analysis and characterization of physiological biodistribution of (⁶⁸Ga-DOTA-TATE PET/CT. *Clin Nucl Med*. 2012;37:1052-7.
- Kuyumcu S, Özkan ZG, Sanli Y, et al. S. Physiological and tumoral uptake of (⁶⁸Ga-DOTATATE: standardized uptake

values and challenges in interpretation. *Ann Nucl Med*. 2013;27:538-45.

- Kabasakal L, Demirci E, Ocak M, et al. Comparison of ⁶⁸Ga-DOTATATE and ⁶⁸Ga-DOTANOC PET/CT imaging in the same patient group with neuroendocrine tumours. *Eur J Nucl Med Mol Imaging*. 2012;39:1271-7.
- Kimura N, Tomizawa S, Arai KN, Kimura N. Chronic treatment with estrogen up-regulates expression of sst2 messenger ribonucleic acid (mRNA) but down-regulates expression of sst5 mRNA in rat pituitaries. *Endocrinology*. 1998;139:1573-80.
- Prasad V, Baum RP. Biodistribution of the Ga-68 labeled somatostatin analogue DOTA-NOC in patients with neuroendocrine tumors: characterization of uptake in normal organs and tumor lesions. *Q J Nucl Med Mol Imaging*. 2010;54:61-7.
- Reynaert H, Rombouts K, Vandermonde A, et al. Expression of somatostatin receptors in normal and cirrhotic human liver and in hepatocellular carcinoma. *Gut*. 2004;53:1180-9.
- Boy C, Heusner TA, Poeppel TD, et al. ⁶⁸Ga-DOTATOC PET/CT and somatostatin receptor (sst1-sst5) expression in normal human tissue: correlation of sst2 mRNA and SUVmax. *Eur J Nucl Med Mol Imaging*. 2011;38:1224-36.
- Reubi JC, Zimmermann A, Jonas S, et al. Regulatory peptide receptors in human hepatocellular carcinomas. *Gut*. 1999;45:766-74.
- Reubi JC, Kappeler A, Waser B, Schonbrunn A, Laissue J. Immunohistochemical localization of somatostatin receptor sst2A in human pancreatic islets. *J Clin Endocrinol Metab*. 1998;83:3746-9.
- Wang X, Zielinski MC, Misawa R, et al. Quantitative analysis of pancreatic polypeptide cell distribution in the human pancreas. *PLoS One*. 2013;8:e55501.
- Reubi JC, Horisberger U, Studer UE, Waser B, Laissue JA. Human kidney as target for somatostatin: high affinity receptors in tubules and vasa recta. *J Clin Endocrinol Metab*. 1993;77:1323-8.
- Gugger M, Waser B, Kappeler A, Schonbrunn A, Reubi JC. Cellular detection of sst2A receptors in human gastrointestinal tissue. *Gut*. 2004;53:1431-6.
- Reubi JC, Horisberger U, Waser B, Gebbers JO, Laissue J. Preferential location of somatostatin receptors in germinal centers of human gut lymphoid tissue. *Gastroenterology*. 1992;103:1207-14.
- Reubi JC, Horisberger U, Kappeler A, Laissue JA. Localization of receptors for vasoactive intestinal peptide, somatostatin, and substance P in distinct compartments of human lymphoid organs. *Blood*. 1998;92:191-7.
- Gugger M, Waser B, Kappeler A, Schonbrunn A, Reubi JC. Immunohistochemical localization of somatostatin receptor sst2A in human gut and lung tissue: possible implications for physiology and carcinogenesis. *Ann N Y Acad Sci*. 2004;1014:132-6.
- Reubi JC, Waser B, Horisberger U, et al. In vitro autoradiographic and in vivo scintigraphic localization of somatostatin receptors in human lymphatic tissue. *Blood*. 1993;82:2143-51.
- Druckenthaner M, Schwarzer C, Ensinger C, et al. Evidence for Somatostatin receptor 2 in thyroid tissue. *Regul Pept*. 2007;138:32-9.
- Oomen SP, Hofland LJ, van Hagen PM, Lamberts SW, Touw IP. Somatostatin receptors in the haematopoietic system. *Eur J Endocrinol*. 2000;143(Suppl 1):9-14.

23. Reubi JC, Schär JC, Waser B, et al. Affinity profiles for human somatostatin receptor subtypes SST1-SST5 of somatostatin radiotracers selected for scintigraphic and radiotherapeutic use. *Eur J Nucl Med*. 2000;27:273-82.
24. Wild D, Schmitt JS, Ginj M, et al. DOTA-NOC, a high-affinity ligand of somatostatin receptor subtypes 2, 3 and 5 for labelling with various radiometals. *Eur J Nucl Med Mol Imaging*. 2003;30:1338-47.
25. Antunes P, Ginj M, Zhang H, et al. Are radiogallium-labelled DOTA-conjugated somatostatin analogues superior to those labelled with other radiometals? *Eur J Nucl Med Mol Imaging*. 2007;34:982-93.